Int J Adv Manuf Technol (2013) 69:439–450
DOI 10.1007/s00170-013-5039-1

ORIGINAL ARTICLE

Determination of flow stress of thin-walled tube based on digital speckle correlation method for hydroforming applications

Jianwei Liu · Xinyu Liu · Lianfa Yang · Huiping Liang

Received: 13 November 2012 / Accepted: 29 April 2013 / Published online: 16 May 2013

Abstract The flow stress, used to describe the plastic deformation behavior of thin-walled tube, is one of the most important parameters to ensure reliable finite element simulation in the tube hydroforming process. In this study, a novel approach of on-line measurement based on digital speckle correlation method is put forward to determine flow stress of thin-walled tube. A simple experimental tooling is developed and free-bulged tests are performed for 304 stainless steel and H62 brass alloy tubes. An analytical approach is proposed according to the membrane theory and the force equilibrium equation. The developed method is validated by means of FE simulations. The results indicate that the present method is acceptable to define the flow stress in the tube hydroforming process.

Keywords Digital speckle correlation method · Tube hydroforming · Flow stress · Finite element simulation

J. Liu
School of Materials Science and Engineering,
Central South University, Changsha 410-083,
People's Republic of China

J. Liu (✉) · H. Liang
Department of Practice Teaching,
Guilin University of Electronic Technology,
Guilin 541-004, People's Republic of China
e-mail: liujianwei78988@163.com

X. Liu
School of Materials Science and Engineering,
Guilin University of Electronic Technology,
Guilin 541-004, People's Republic of China

L. Yang
School of Mechanical and Electrical Engineering,
Guilin University of Electronic Technology,
Guilin 541-004, People's Republic of China

1 Introduction

Tube hydroforming (THF) has been widely used in automotive and aircraft industries, household appliances and other components, because of many remarkable advantages compared to conventional stamping processes, such as weight reduction, improved structural strength and stiffness, tight dimensional tolerances, low spring back, and high geometry accuracy [1–3]. Nonetheless, the THF process suffers from some disadvantages such as slow production cycle and expensive tooling. In order to shorten the trial and error phases which are time- and cost-consuming, finite element (FE) simulation of the THF process has been used gradually during the last few decades. However, the reliable FE simulation must depend on an accurate knowledge of material properties, especially flow stress [4–6].

Many studies on the flow stress of thin-walled tube have been reported in recent years. Tensile test is the most common and simplest method. The parameters of flow stress are derived from the testing data of the flat sheets used to manufacture the tubes. However, the accuracy and appropriateness of tensile test results for the THF is questionable due to the facts that (a) the tensile test is under uni-axial loading, but the THF is under bi-axial or tri-axial loading, (b) the material properties, obtained from the flat sheets prior to rolling and welding operations, are altered inevitably during manufacturing process of the tube [7].

For the reasons stated above, the tube bulge test has been proposed to determine the flow stress of thin-walled tube. Koç et al. [7] and Bortot et al. [8] put forward a method of "on-line" measurement to determine the flow stress. The tubular bulge parameters were measured by some sophisticated measurement techniques, such as coordinate measuring machine. The stresses and strains were calculated through the force equilibrium and incremental theory. Tian et al. [9] adopted THF process, uni-axial compression test

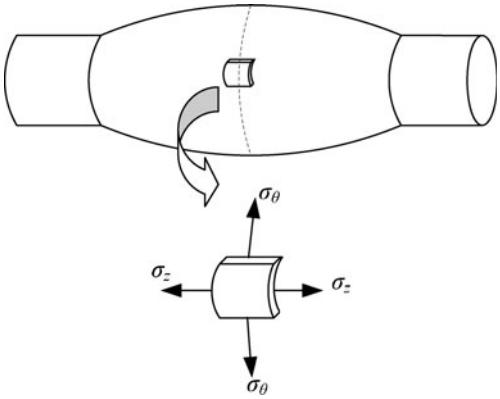

Fig. 1 Stress state at the bulge tip

and least-squares fitting technique to estimate the flow stress of tubular material based on the isotropic hardening assumption. Hwang et al. [10] and Lin et al. [11] deduced mathematical model for meridian radius and thickness distribution based on the assumption of elliptical surface in the middle free bulge region. Strano et al. [12] founded an inverse approach based on the energy balance to determine the flow stress of thin-walled tube. Yang et al. [13] set up the stress–strain relationship of a thin-walled tube based on the plastic membrane theory, force equilibrium equations and curve fitting of experimental data. Song et al. [14] obtained the circumferential and axial stress at the maximum bulge element in tubular blank using the force equilibrium.

However, some disadvantages of these researches stated above are (a) lots of methods assumed a bulge profile such as circular arc, elliptical arc and cosine curve, but experiments showed the real profile of bulge was uncertain, (b) these geometrical data, for instance the thickness, gage length, longitudinal and circumferential radius, was obtained from off-line measuring different tubes with the increasing of internal pressure, so the process in which several tubes were measured resulted in the low accuracy, (c) the "on-line" method, using coordinate measuring machine to obtain bulge shape, was feasible but very expensive and sophisticated.

In this paper, analytical approach is proposed on the basis of the force equilibrium equation. A unique on-line measurement approach based on digital speckle correlation method is put forward to determine flow stress of thin-walled tube in THF process.

2 Analytical approach

2.1 Equivalent stress σ_e

In this study, the thickness of tube is very small compared to the external diameter, so the stress in the thickness direction (σ_t) is ignored. Figure 1 shows the state of stress at the top of the dome during the bulge test. According to the membrane theory and the force equilibrium equation for an element, the equation can be expressed by

$$\sigma_z \Big/ r_z + \sigma_\theta \Big/ r_\theta = P \Big/ t \tag{1}$$

where σ_z and σ_θ are the axial and circumferential stress, r_z and r_θ are the longitudinal and circumferential radius, P and t are the internal pressure and thickness, respectively.

According to the force equilibrium in axial direction of tube, the equation can be written as

$$P\left(\pi r_\theta^2 - \pi r_0^2\right) - \sigma_z (2\pi r_\theta t) = F_a + F_S - F_f \tag{2}$$

where r_0 is the initial radius, F_a, F_f and F_s are the feeding force in axial direction, friction force between bulge dies and tubular blank, and sealing force against pressurized

Fig. 2 THF apparatus

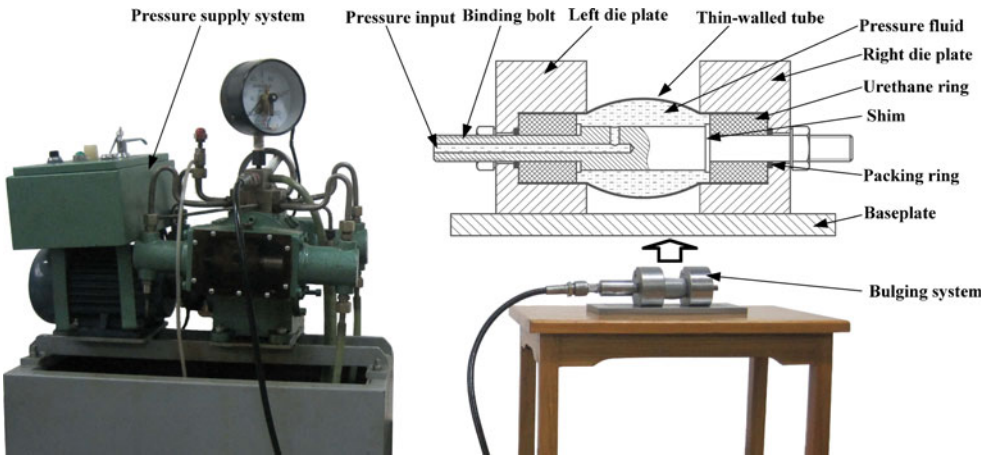

Fig. 3 3D digital speckle analysis system

fluid, respectively. In the test, the axial force F_a is not taken into account, and the friction force F_f is neglected because it is considered negligible compared to F_s. The sealing force F_s can be expressed as the following equation

$$F_s = P\pi(r_0 - t_0)^2 \tag{3}$$

where t_0 means the initial thickness of the tube. The force equilibrium in axial direction of tubular blank can be quoted from Eqs. (2) and (3)

$$P\left(\pi r_\theta^2 - \pi r_0^2\right) - \sigma_z(2\pi r_\theta t) = P\pi(r_0 - t_0)^2 \tag{4}$$

From Eqs. (1) and (4), the axial and circumferential stress can be calculated as

$$\sigma_\theta = r_\theta\left(P\Big/t - \sigma_z\Big/r_z\right) \tag{5}$$

$$\sigma_z = P\left(r_\theta^2 - r_0^2 - t_0^2 + 2r_0t_0\right)\Big/(2r_\theta t) \tag{6}$$

Finally, according to the Von-Mises yield criterion for the plane stress condition, the equivalent stress can be deduced as

$$\sigma_e = \sqrt{\sigma_z^2 - \sigma_z\sigma_\theta + \sigma_\theta^2} \tag{7}$$

Table 1 Initial conditions used in the experiment of the free hydraulic bulge

Parameter	Value (mm)
Initial wall thickness t_0	0.6
Initial tube radius r_0	16
Total length of tube L	110
Gage length l_0	50

2.2 Equivalent strain ε_e

The calculated circumferential ε_θ and thickness ε_t strains at the top of the dome can be expressed as

$$\varepsilon_\theta = \ln\left(r_\theta\Big/r_0\right), \quad \varepsilon_t = \ln\left(t\Big/t_0\right) \tag{8}$$

The calculated axial strain ε_z can be determined under the assumption of constant volume and neglect of elastic strain by

$$\varepsilon_z + \varepsilon_\theta + \varepsilon_t = 0 \tag{9}$$

Therefore, the equivalent strain is deduced as

$$\varepsilon_e = \sqrt{\frac{4}{3}\left(\varepsilon_\theta^2 + \varepsilon_\theta\varepsilon_t + \varepsilon_t^2\right)} \tag{10}$$

2.3 Flow stress equation

Through several experiments using different internal pressures, it is possible to obtain a series of (σ_e, ε_e) couples representing the stress–strain relationship of the tube. These values, plotted in a σ_e–ε_e diagram, can be fitted by means of the Hollomon hardening rule, so obtaining the flow stress equation on behalf of the material behavior as following

$$\sigma_e = K\varepsilon_e^n \tag{11}$$

where K and n are the strength coefficient and work hardening exponent, respectively.

3 Experimental tooling and procedure

3.1 Experimental tooling

In order to obtain experimental data to determine the flow stress of thin-walled tube, a simple and practical tooling has been

developed. The basic system of the experimental tooling is comprised of a THF apparatus and a measuring device.

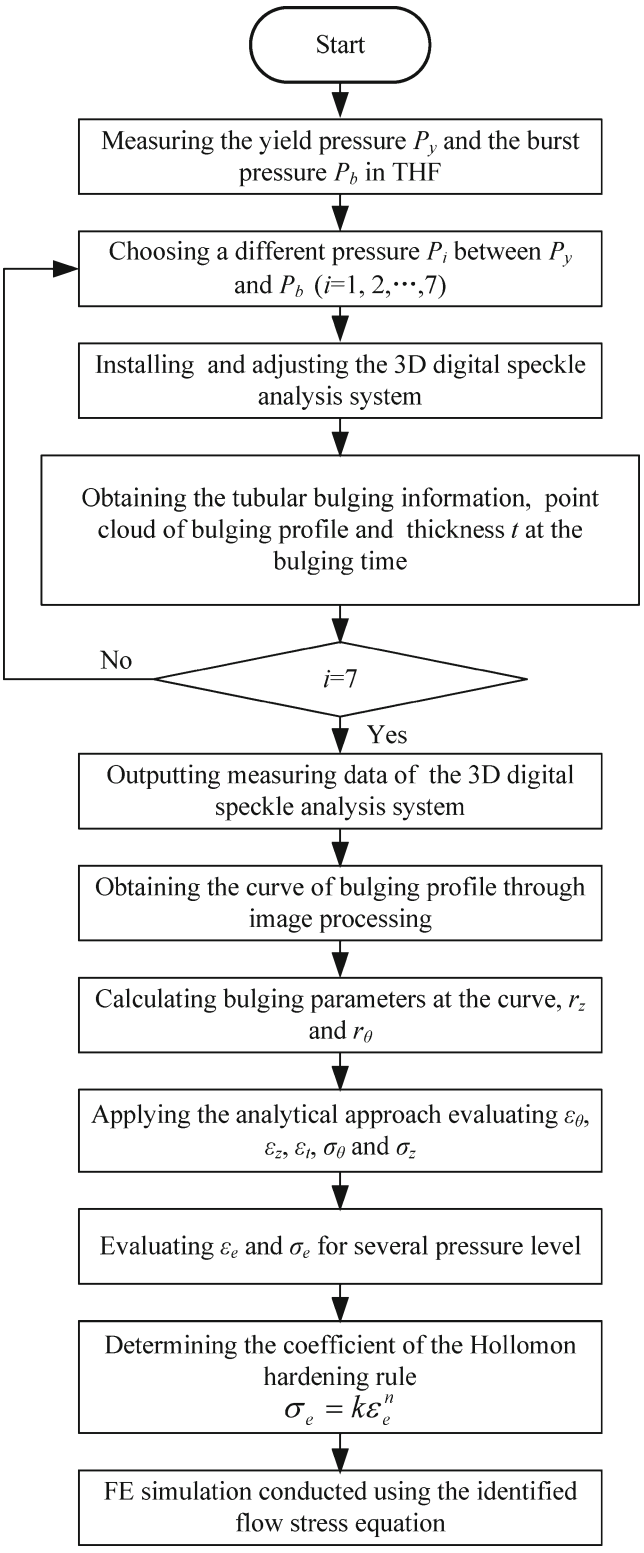

Fig. 4 Flow chart of experimental procedure determining flow stress

(1) THF apparatus

The THF apparatus for bulge experiments is composed of two parts, pressure supply system and bulging system, as shown in Fig. 2.

The pressure supply system provides and controls the internal hydraulic pressure. The pressure fluid is compressed into the tube through pressure input of binding bolt. The system is designed and machined for a pressure gage and a pressure relief valve in order to measure and control promptly the fluid pressure.

The bulging system is designed to be a stand-alone unit. The left and right die plates are held together by binding bolt. The tube is contained by left and right die plates. The outside diameter and bulge length of tube are confined respectively by the inside diameter of die plates and length of binding bolt. To ensure the tightness of tube, the ends of the tube are pressed against the internal surfaces of these dies by urethane rings. Moreover, the packing rings outside the tube can cause a tighter sealing.

(2) Measuring device

To obtain the bulge parameters, including the circumferential radius r_θ, longitudinal radius r_z and thickness t, the digital speckle correlation method (DSCM) is adopted.

The DSCM is an advanced experimental stress analysis technology which shows special advantages in deformation measurement of test specimen, for instance non-contact, having simple optical set-up, no special preparation for the specimen, no special requirement for test environment, and so on. Therefore, it has been widely used in many researches and engineering applications to obtain the surface deformation fields [15].

In this study, the 3D digital speckle analysis system for dynamic strain measurement, which has been developed at Xi'an Jiaotong University of China, is introduced for acquiring bulge parameters. Figure 3 shows the main components of the 3D digital speckle analysis system, which consist of the following parts: (1) two CMOS cameras, used to record the speckle image of the specimen with a resolution of 1280×960 pixels, (2) two high-frequency LED lights for illumination, (3) a control box for dominating the cameras and LED lights, (4) a tripod for supporting, and (5) a computer for installing software [16, 17].

3.2 Experimental material and procedure

Two kinds of tubular materials, 304 stainless steel and H62 brass alloy, are investigated during validation of this project.

Table 2 Internal pressure used in experimental investigation of 304 stainless steel and H62 brass alloy tubes

Tube material	Pressure level (MPa)								
	P_y	P_1	P_2	P_3	P_4	P_5	P_6	P_7	P_b
304 stainless steel	15.2	20	21	22	23	24	25	26	27.4
H62 brass alloy	3.3	4	5	6	7	8	9	-	9.4

The initial conditions used in the experiment are shown in Table 1.

Figure 4 shows procedure of the experiments based on digital speckle correlation method to determine the flow stress of tubular material for THF.

(1) Choosing internal pressures of experiments

Initial experiments are carried out to determine the two critical internal pressures, the yield pressure P_y and the burst pressure P_b in the free-bulged tests. As the bulge parameters are measured "online" using the 3D digital speckle analysis system, tube free-bulged experiments are preformed to the same tube with different pressure levels between P_y and P_b. In tests, several pressure levels are chosen to obtain the equivalent stress–strain relationship as shown in Table 2.

(2) Installing and calibrating the experimental tooling

The CMOS cameras and high-frequency LED lights are installed on tripod. The cameras should be calibrated when they are used for the first time or the relative position is changed in order to obtain the interior orientation parameters and the lens distortion parameters. Figure 5 shows the calibration target with 17 coded points and 126 uncoded points. In the calibration, the target is placed 1,000 mm from the measurement device, and captured eight pairs of images in different locations by moving it, as shown in Fig. 6. The 17 coded points should be shown clearly through adjusting measurement device at each location.

Owing to no obvious feature, the tube surface is sprayed stochastic speckle, as shown in Fig. 7. Then, the tube is embedded correctly in the THF apparatus. Simultaneously, two cameras should aim at the bulge region to acquire image, as shown in Fig. 8.

(3) Obtaining the tubular bulge information

The images are captured by the cameras during the deformation, and the calculation area is selected in the left image of the first stage and some seed points are adopted to calculate all the points accurately and quickly, as shown in Fig. 9. Then, all the other images are processed using the digital speckle correlation method, and corresponding points in all the stages are obtained. At last, the tubular bulge information, such as the 3D coordinates of all the points and thickness reduction (t_i'), is output in time. The radial direction displacement field and thickness reduction of a state point are shown in Figs. 10 and 11, respectively.

(4) Defining bulge profile curves and equations

According to the 3D coordinates of all the points, bulge profiles are obtained through UG software under different internal pressures, as shown in Fig. 12. Because different calculation areas are selected on the bulge tube, the bulge profiles are not symmetrical completely. Then, fitting smooth curves through the coordinate are conducted by using MATLAB. Its mathematic formula is expressed by

$$y = f(x) = a_0 + a_1 x + a_2 x^2 + \cdots + a_n x^n \tag{12}$$

where y is the circumferential radius of bulge profile at each internal pressure, x is the axial location, a_0, a_1, a_2, and a_n are the equation coefficients. The results of a_0,

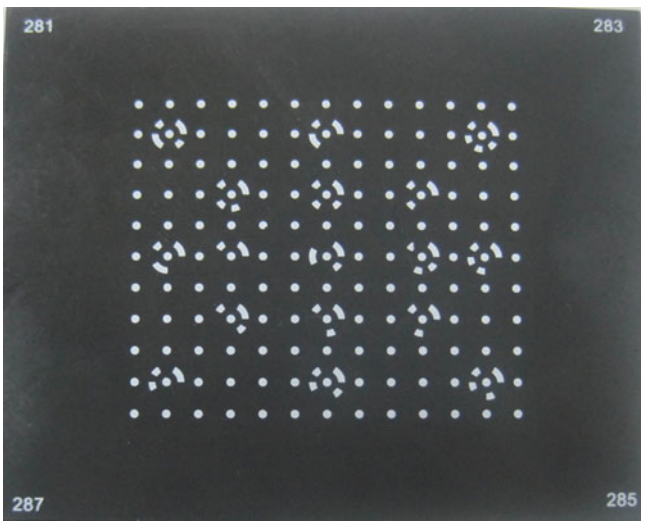

Fig. 5 Calibration target

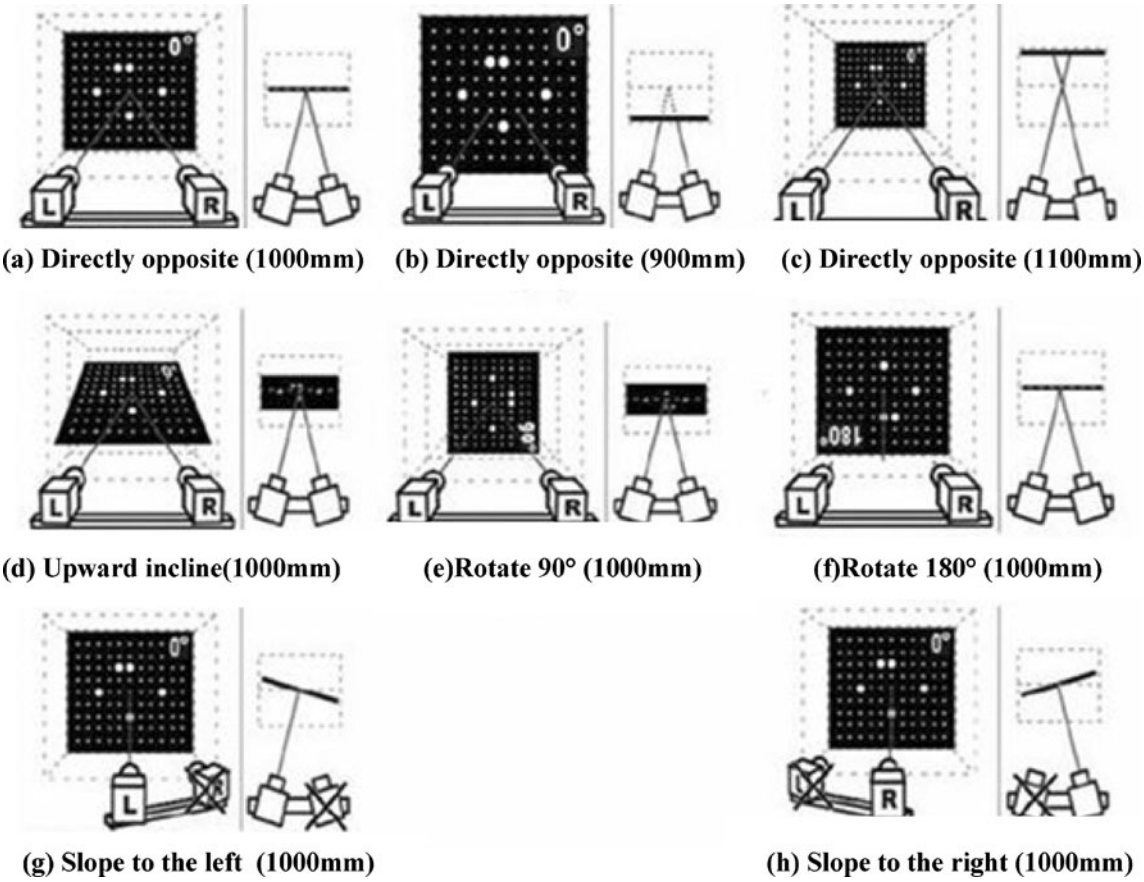

Fig. 6 Calibrating method

a_1 and a_2 are shown in Table 3. The other equation coefficients are too small to be considered.

(5) Calculating bulge parameters

Making use of the bulge equations, circumferential radius r_θ and longitudinal radius r_z are calculated as follows

$$r_\theta = y_{\max} = \left| \left(4a_0a_2 - a_1^2\right) \Big/ \left(4a_2\right) \right| \tag{13}$$

$$r_z = \left| \left[1 + \left(dy \Big/ dx \right)^2 \right]^{3/2} \Big/ \left(d^2y \Big/ dx^2 \right) \right|_{x=-a_1/(2a_2)} \tag{14}$$

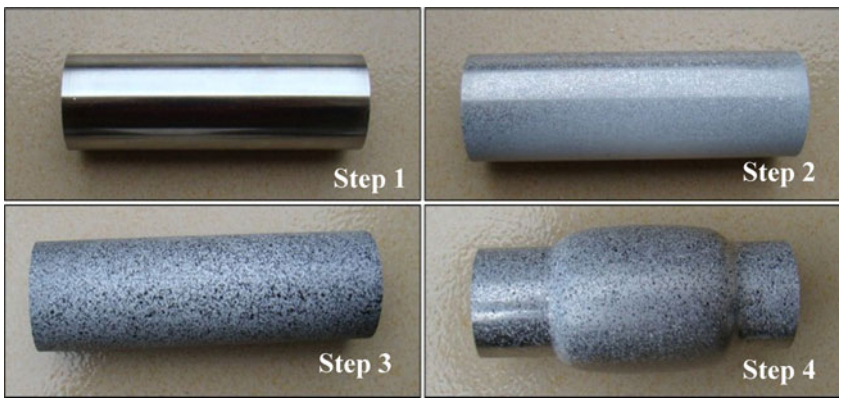

Fig. 7 The procedure of spraying stochastic speckle in the tube surface, *step 1* is original tube, *step 2* is tube with write spray, *step 3* is tube with black spray, and *step 4* is bulge tube

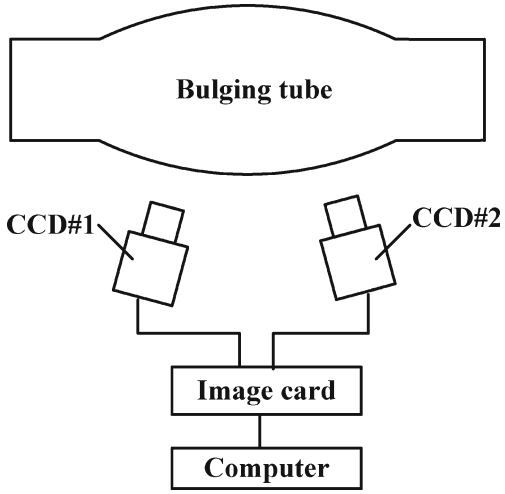

Fig. 8 Schematic of test system of THF

And t can be expressed as

$$t = t_0 - t_i, \quad t_i = \max\left(t_i'\right) \quad (i = 1, 2, 3 \ldots 7) \tag{15}$$

where t_i and t_i' are the maximum thickness reduction and thickness reduction under different internal pressures, respectively. t_i' can be obtained directly from output information of the measurement system. The results are shown in Table 4.

(6) Evaluating equivalent stress and strain

Using the analytical approach in Section 2, the axial stress σ_z, circumferential stress σ_θ, circumferential true strain ε_θ , radius true strain ε_t, equivalent strain ε_e and equivalent stress σ_e can be evaluate one by one, as shown in Table 5.

(7) Determining the flow stress curve

The parameters of the strength coefficient K and the work hardening exponent n can be defined by fitting a series of (σ_e, ε_e) couples to Eq. (11) via MATLAB least-squares fitting methods. The flow stress curves are obtained as shown in Fig. 13.

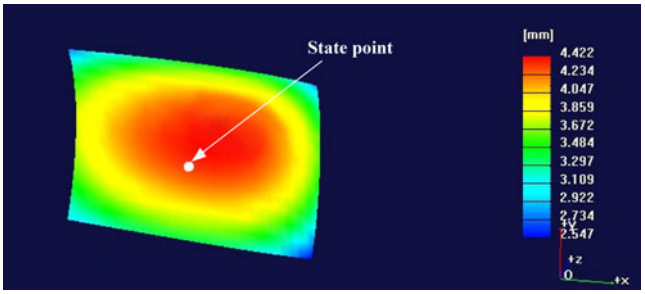

Fig. 10 Radial direction displacement field

3.3 Validation of the developed approach

In order to validate the developed approach, FE simulations of the free hydraulic bulge have been performed using a dynamic explicit commercial FE code "DYNAFORM". Figure 14 shows the geometrical FE model, where the x-axis denotes the axial direction of the tube. The edge of the tubular blank can be moved freely. Contact between the tube and die is modeled using a friction coefficient of μ=0.125. The tubular material is assumed to be isotropic, homogeneous and incompressible in deformation.

The flow chart to validate the approach is shown in Fig. 15. The strength coefficient K and work hardening exponent n, obtained from the developed approach, are input into FE simulations. Then, the thickness t, longitudinal radius r_θ and circumferential radius r_z at the top of the dome can be obtained from FE simulation at several internal pressures. At last, the flow stress is determined using the approach in Section 2. If the developed approach is correct, the flow stress is obtained by using the FE simulations

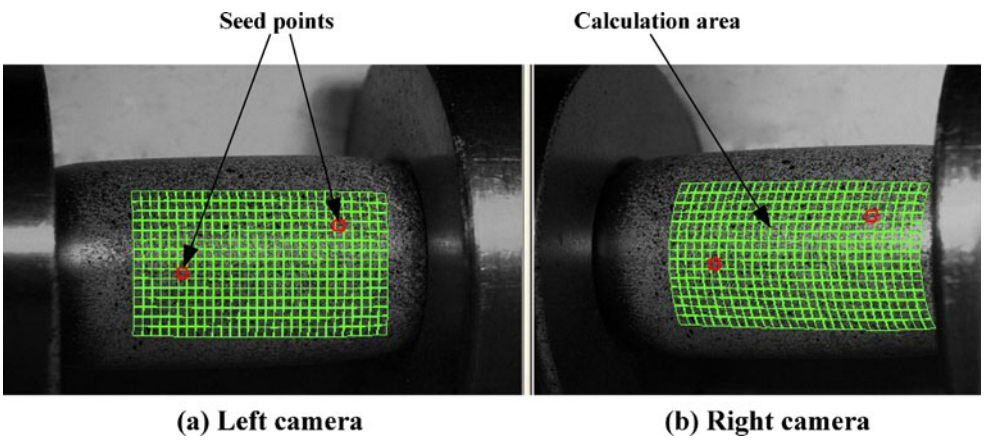

Fig. 9 Image matching based on seed points in the calculation area, **a** left camera and **b** right camera

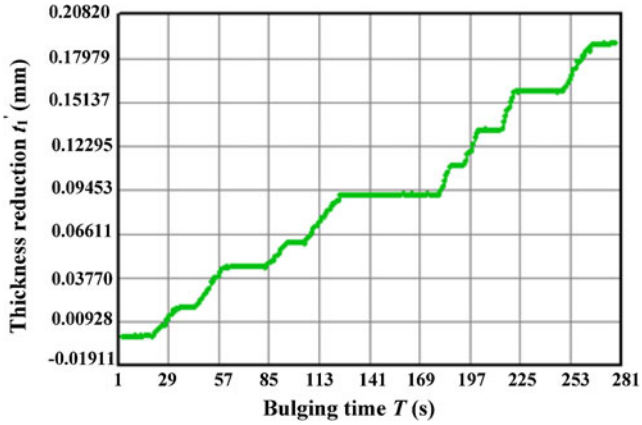

Fig. 11 Thickness reduction of a state point along with the process of THF

should be as close as possible to the result of experiments. Furthermore, the bulge parameters, such as the thickness t and circumferential radius r_θ, should show a good agreement.

Figure 16 shows the comparison of the circumferential radius r_θ and thickness t between the experiments and the FE simulations for 304 stainless steel tube. At several internal pressure levels, the discrepancies of the circumferential radius r_θ are in the range of 10 %, and a good agreement is obtained, except for the pressure level P_3=22 MPa, where the measured error is about 11 %. For the thickness values the discrepancies are in the range of 5 %, and a good agreement is obtained too. The difference is due to the fact that simulations are performed on a perfect geometry

Fig. 12 Bulge profiles obtained from experiment

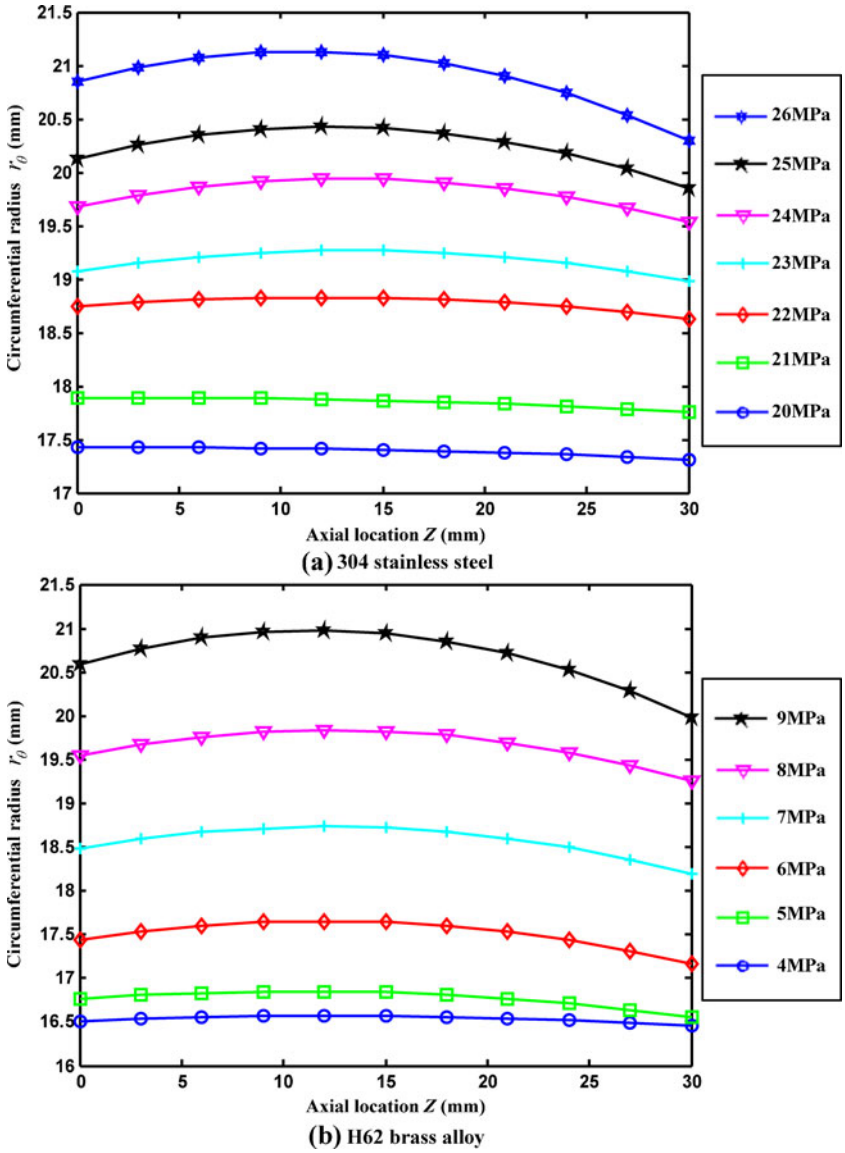

Table 3 Coefficient of equation obtained by using MATLAB for 304 stainless steel and H62 brass alloy tubes

304 stainless steel				H62 brass alloy			
Pressure (MPa)	a_0	a_1	a_2	Pressure (MPa)	a_0	a_1	a_2
20	17.425	0.00082	−0.00015	4	16.5079	0.0102	−0.0004
21	17.889	0.00103	−0.00018	5	16.7635	0.0169	−0.0008
22	18.738	0.01493	−0.00062	6	17.4428	0.0358	−0.0015
23	19.071	0.02905	−0.00107	7	18.4829	0.0414	−0.0017
24	19.68	0.03865	−0.00144	8	19.5476	0.0471	−0.0019
25	20.128	0.04707	−0.00188	9	20.5931	0.0667	−0.0029
26	20.844	0.05205	−0.00235	–	–	–	–

Table 4 Bulge parameters at several internal pressure levels for 304 stainless steel and H62 brass alloy tubes

Tube material	Pressure (MPa)	x (mm)	r_θ (mm)	r_z (mm)	t (mm)
304 stainless steel	20	2.7252	17.4261	3311.258	0.5656
	21	2.79	17.8904	2711.644	0.548
	22	12.0082	18.8276	804.2982	0.5154
	23	13.5523	19.2678	466.5485	0.5013
	24	13.3739	19.9384	346.0447	0.4797
	25	12.5156	20.4226	265.8867	0.4582
	26	11.0782	21.1323	212.8203	0.4332
H62 brass alloy	4	12.75	16.5729	1250	0.5794
	5	10.5625	16.8528	625	0.5507
	6	11.9333	17.6564	333.3333	0.5194
	7	12.1765	18.735	294.1176	0.483
	8	12.3947	19.8395	263.1579	0.4183
	9	11.5	20.9766	172.4138	0.3412

Table 5 Stress and strain at several internal pressure levels

Tube material	Pressure (MPa)	ε_θ	ε_t	σ_z (MPa)	σ_θ (MPa)	σ_e (MPa)	ε_e
304 stainless steel	20	0.0854	−0.0756	67.7924	615.8427	584.9010	0.0934
	21	0.1117	−0.1072	89.1236	684.9944	645.0670	0.1264
	22	0.1627	−0.1685	133.3410	800.5420	742.9010	0.1913
	23	0.1859	−0.1963	160.0140	877.4135	809.3580	0.2209
	24	0.2201	−0.2403	201.6080	985.9291	902.1810	0.2666
	25	0.2441	−0.2862	240.7520	1095.7900	997.4490	0.3090
	26	0.2782	−0.3423	297.8200	1238.7580	1119.9500	0.3639
H62 brass alloy	4	0.0352	−0.0349	7.8110	114.3108	110.6124	0.0405
	5	0.0519	−0.0857	12.6215	152.6718	146.7686	0.0864
	6	0.0985	−0.1443	24.4000	202.6707	191.6392	0.1474
	7	0.1578	−0.2169	44.0309	268.7163	249.6305	0.2243
	8	0.2151	−0.3607	75.4058	373.7461	342.3296	0.3630
	9	0.2708	−0.5645	127.5445	537.7931	486.7201	0.5646

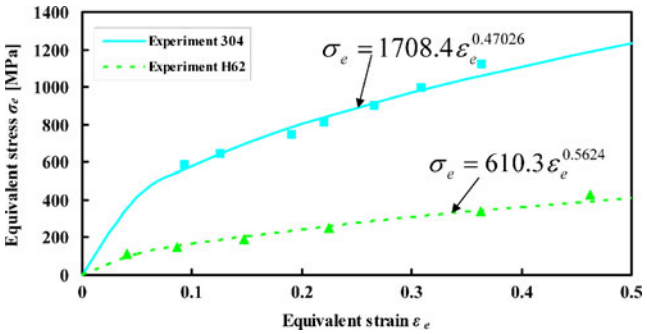

Fig. 13 Flow stress curves obtained by digital speckle correlation method in THF

without local neck by assuming that the tube is isotropic, homogeneous, and axisymmetric deformation during the whole bulge. On the other hand, obtaining the curves of bulging profile, from measuring data of the 3D digital speckle analysis system, might lead to some errors.

Figure 17 shows the comparison of the circumferential radius r_θ and thickness t between the experiments and the FE simulations for H62 brass alloy tube. For the circumferential radius, r_θ, the discrepancies are in the range of 6 %, and a good agreement is obtained. For the thickness, t, the measured errors are in the range of 10 %, except for the last point, corresponding at the burst pressure, where the error is 11.4 %. The difference is due to the localized neck is formed and the unstable deformation occurs at the last point. A small increase of the pressure can cause a high deformation at this moment. But the situation does not occur in the FE simulation because the material is considered as isotropic and homogeneous deformation during the whole bulge.

The stress–strain relationship is obtained from the FE simulation using the approach in Section 2. Figure 18 shows the comparison of flow stress between the experiment and FE simulation for 304 stainless steel and H62 brass alloy tube. It can be seen that the flow stress curves of FE

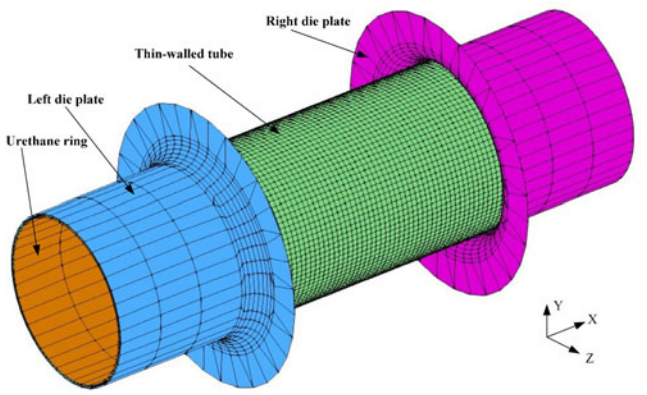

Fig. 14 Geometrical FE model for free hydraulic bulge

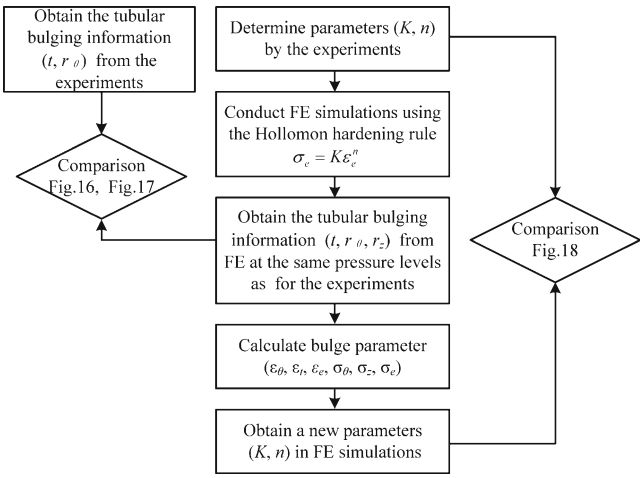

Fig. 15 Flow chart for validating the developed approach

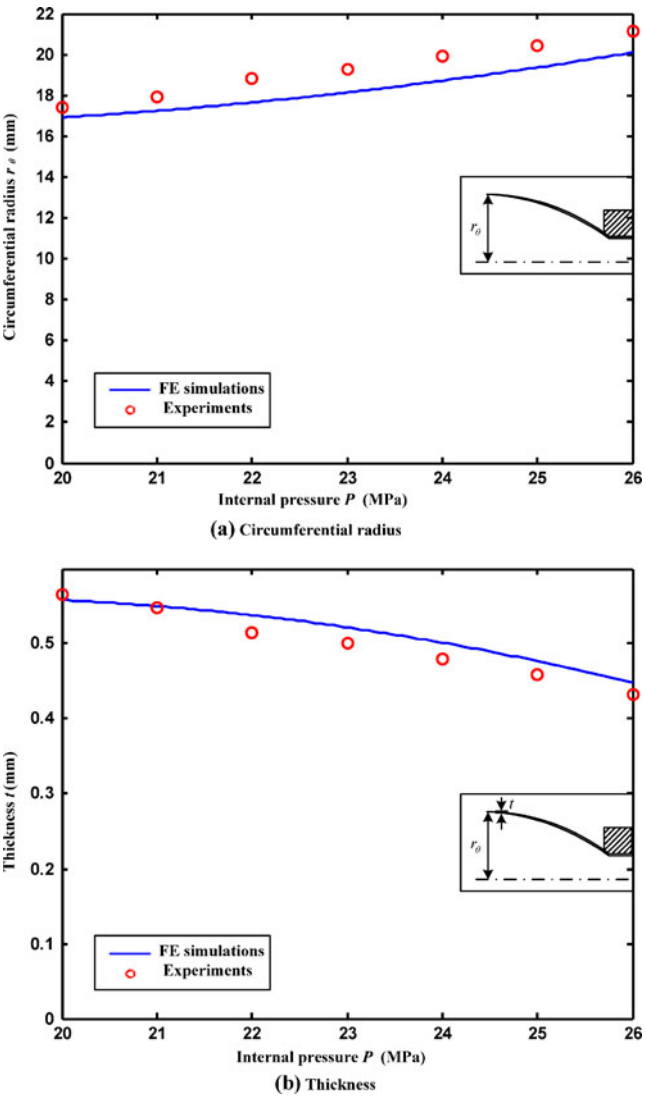

Fig. 16 Comparison of **a** circumferential radius and **b** thickness between the experiments and FE simulations in all internal pressures for 304 stainless steel tube

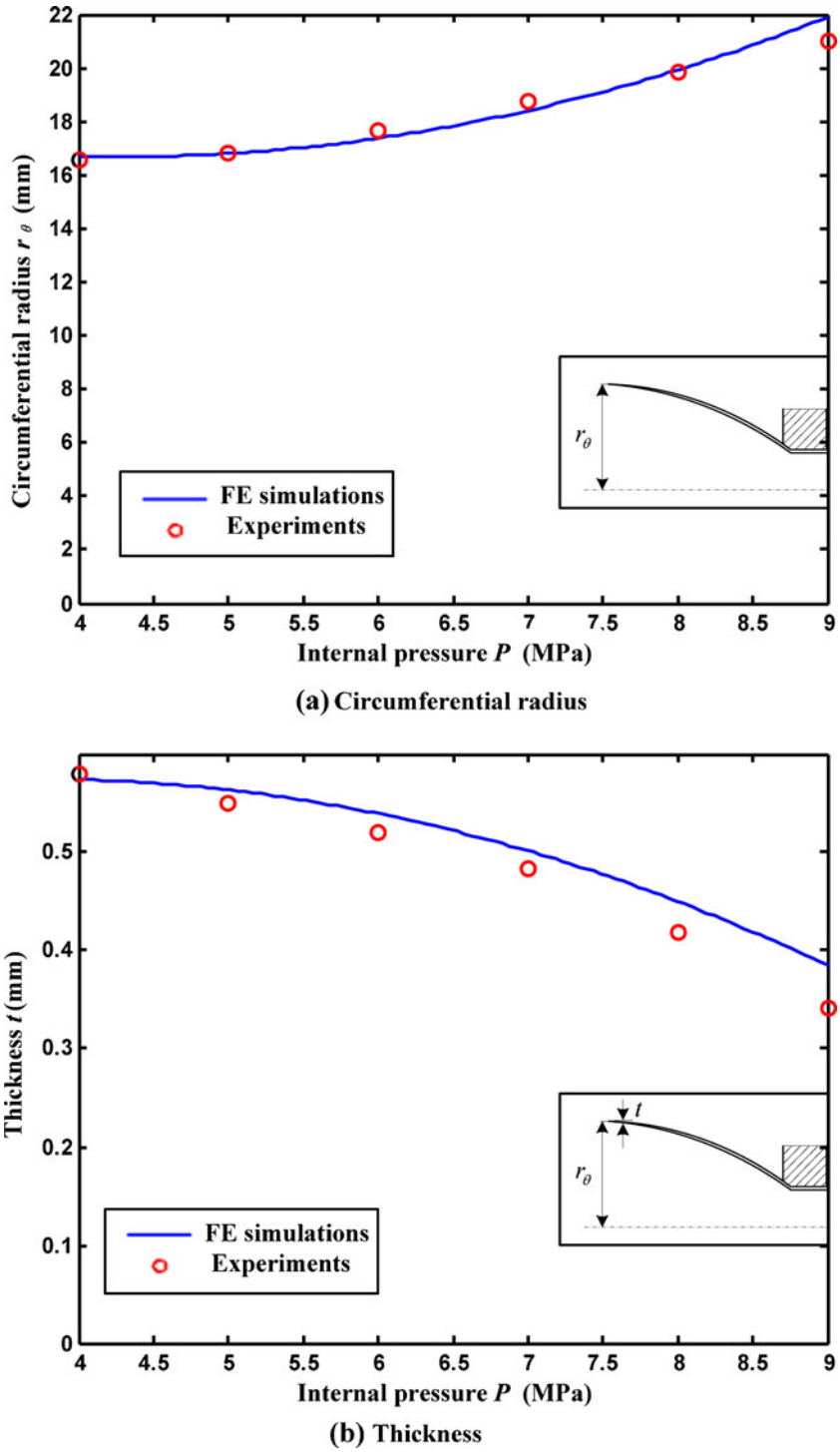

Fig. 17 Comparison of **a** circumferential radius and **b** thickness between the experiments and FE simulations in all internal pressures for H62 brass alloy tube

simulation are very close to the results of experiments. For the 304 stainless steel tube, the measuring errors of the strength coefficient K and work hardening exponent n are in the range of 5.0 and 8.6 %, respectively. For the H62 brass alloy, the measuring errors of the strength coefficient K and work hardening exponent n are in the range of 3.4 and 2.4 %, respectively. Because formability of the H62 brass alloy tubes is enhanced evidently by rime annealing at 650 °C, the flow stress curve of the FE simulation is slightly higher than the experiment.

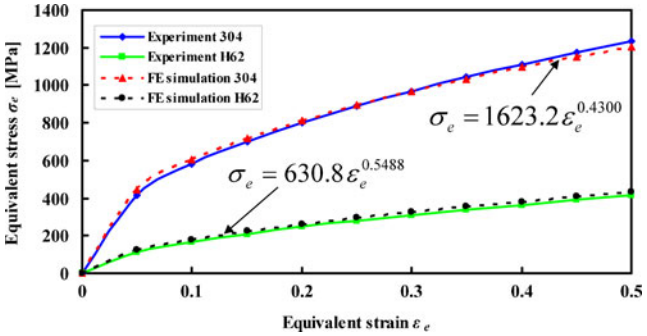

Fig. 18 Comparison of flow stress between the experiments and the FE simulations for 304 stainless steel and H62 brass alloy tube

4 Conclusions

The paper has proposed a unique approach to determine the flow stress of tubular material for THF applications based on digital speckle correlation method. A simple and practical experimental tooling, the THF apparatus and measuring device, has been developed, by which the bulge parameters are conveniently obtained "on-line". The stress–strain distribution is deduced at several internal pressure levels with a reasonable analytical approach according to the force equilibrium equation. By means of the Hollomon hardening rule, these experimental values on equivalent stress and strain are fitted and the flow stress equation is defined.

The approach is validated by the FE simulation conducted with the calculated flow stress equation. The comparisons of circumferential radius, thickness, and flow stress relationship between the FE simulation and the experiments show a good agreement.

In future work, analytical approaches considering axial-feeding force and friction force between bulge dies and tubular blank will be developed.

Acknowledgments The authors gratefully acknowledge the supports of the National Natural Science Foundation of China (Grant no: 51065006 and 51271062) and the Guangxi Natural Science Foundation (Grant no: 2013GXNSFAA019245).

References

1. Aueulan Y, Ngaile G, Altan T (2004) Optimizing tube hydroforming using process simulation and experimental verification. J Mater Process Technol 146:137–143. doi:10.1016/S0924-0136(03)00854-9
2. Mohammadi F, Mashadi MM (2009) Determination of the loading path for tube hydroforming process of a copper joint using a fuzzy controller. Int J Adv Manuf Technol 43:1–10. doi:10.1007/s00170-008-1697-9
3. Elie-dit-cosaque X, Chebbah MS, Naceur H, Gakwaya A (2012) Analysis and design of hydroformed thin-walled tubes using enhanced one-step method. Int J Adv Manuf Technol 59:507–520. doi:10.1007/s00170-011-3539-4
4. Alaswad A, Benyounis KY, Olabi AG (2012) Tube hydroforming process: a reference guide. Mater Des 33:328–339. doi:10.1016/j.matdes.2011.07.052
5. Strano M, Jirathearanat S, Shr SG, Altan T (2004) Virtual process development in tube hydroforming. J Mater Process Technol 146:130–136. doi:10.1016/S0924-0136(03)00853-7
6. Chen XF, Li SH, Yu ZQ, Lin ZQ (2012) Study on experimental approaches of forming limit curve for tube hydroforming. Int J Adv Manuf Technol 61:87–100. doi:10.1007/s00170-011-3707-6
7. Koç M, Aueulan Y, Altan T (2001) On the characteristics of tubular materials forhydroforming—experimentation and analysis. Int J Mach Tools Manuf 41:761–772
8. Bortot P, Ceretti E, Giardini C (2008) The determination of flow stress of tubular material for hydroforming applications. J Mater Process Technol 203:381–388. doi:10.1016/j.jmatprotec.2007.10.047
9. Tian ZK, Ma ZE (2002) Estimation of the hardening characteristics of tubular material. Mechanical science and technology 3:272–273 (in Chinese)
10. Hwang YM, Lin YK (2002) Analysis and finite element simulation of the tube bulge hydroforming process. J Mater Process Technol 125:821–825
11. Lin YL, He ZB, Yuan SJ (2010) The factors affecting the profile of middle bulge region during tube bulge test. Acta Metallurgica Sinica 6:729–735 (in Chinese)
12. Strano M, Altan T (2004) An inverse energy approach to determine the flow stress of tubular materials for hydroforming applications. J Mater Process Technol 146:92–96. doi:10.1016/j.jmatprotec.2003.07.016
13. Yang LF, Guo C (2008) Determination of stress–strain relationship of tubular material with hydraulic bulge test. Thin-Walled Struct 46:147–154. doi:10.1016/j.tws.2007.08.017
14. Song WJ, Kim J, Kang BS (2007) Experimental and analytical evaluation on flow stress of tubular material for tube hydroforming simulation. J Mater Process Technol 191:368–371. doi:10.1016/j.jmatprotec.2007.03.034
15. Meng LB, Jin GC, Yao XF, Yeh HY (2006) 3D full-field deformation monitoring of fiber composite pressure vessel using 3D digital speckle correlation method. Polym Test 25:42–48
16. Tang ZZ, Liang J, Xiao ZZ, Guo C, Hu H (2010) Three-dimensional digital image correlation system for deformation measurement in experimental mechanics. Opt Eng 10:1–9
17. Koç M, Billur E, Cora ÖN (2011) An experimental study on the comparative assessment of hydraulic bulge test analysis methods. Mater Des 32:272–281. doi:10.1016/j.matdes.2010.05.057